Pain Medicine

Pain Medicine 2014; 15: 93–110
Wiley Periodicals, Inc.

TRANSLATIONAL RESEARCH SECTION

Original Research Article

Analgesic Efficacy and Mode of Action of a Selective Small Molecule Angiotensin II Type 2 Receptor Antagonist in a Rat Model of Prostate Cancer-Induced Bone Pain

Arjun Muralidharan, PhD,*† Bruce D. Wyse, PhD,*† and Maree T. Smith, PhD*†

*Centre for Integrated Preclinical Drug Development and

†The School of Pharmacy, The University of Queensland, Brisbane, Queensland, Australia

Reprint requests to: Maree T. Smith, PhD, Centre for Integrated Preclinical Drug Development, Level 3, Steele Building, St Lucia Campus, Brisbane, QLD 4072, Australia. Tel: +61-7-33652554; Fax: +61-7-33467391; E-mail: maree.smith@uq.edu.au.

Disclosures: Arjun Muralidharan was supported by an International PhD Scholarship funded by The University of Queensland, and this project was supported by research funds from The University of Queensland. This work utilized facilities funded by the Queensland Government Smart State Research Facilities Fund. MTS and BDW are named inventors on a UQ patent for the use of AT_2R antagonists in neuropathic pain, and MTS is a named inventor on a UQ patent for the use of AT_2R antagonists in inflammatory pain. This technology is being commercialized by the UQ spin-out company, Spinifex Pharmaceuticals Pty Ltd. UQ owns shares in Spinifex Pharmaceuticals Pty Ltd, and according to UQ policy, inventors will receive a portion of any net income received by UQ in the event of successful commercialization.

Abstract

Objective. The pathobiology of prostate cancer (PCa)-induced bone pain (PCIBP) has both inflammatory and neuropathic components. Previously, we showed that small molecule angiotensin II type 2 receptor (AT_2R) antagonists with >1,000-fold selectivity over the angiotensin II type 1 receptor produced dose-dependent analgesia in a rat model of neuropathic pain. Here, we assessed the analgesic efficacy and mode of action of the AT_2R antagonist, EMA200, in a rat model of PCIBP.

Methods. At 14–21 days after unilateral intratibial injection of AT3B PCa cells, rats exhibiting hindpaw hypersensitivity received single intravenous bolus doses of EMA200 (0.3–10 mg/kg) or vehicle, and analgesic efficacy was assessed. The mode of action was investigated using immunohistochemical, Western blot, and/or molecular biological methods in lumbar dorsal root ganglia (DRGs) removed from drug-naïve and EMA200-treated PCIBP rats relative to sham-control rats.

Results. Intravenous bolus doses of EMA200 produced dose-dependent analgesia in PCIBP rats. Lumbar DRG levels of angiotensin II, nerve growth factor (NGF), tyrosine kinase A (TrkA), phospho-p38 mitogen-activated protein kinase (MAPK), and phospho-p44/p42 MAPK, but not the AT_2R, were increased significantly ($P < 0.05$) in PCIBP rats, c.f. the corresponding levels for sham controls. EMA200 produced analgesia in PCIBP rats by reducing elevated angiotensin II levels in the lumbar DRGs to attenuate augmented angiotensin II/AT_2R signaling. This in turn reduced augmented NGF/TrkA signaling in the lumbar DRGs. The net result was inhibition of p38 MAPK and p44/p42 MAPK activation.

Conclusion. Small molecule AT_2R antagonists are worthy of further investigation as novel analgesics for relief of intractable PCIBP and other pain types where hyperalgesia worsens symptoms.

Key Words. Prostate Cancer-Induced Bone Pain (PCIBP); Angiotensin II; Angiotensin II Type 2 Receptor (AT_2R); Phospho-p38 Mitogen-Activated Protein Kinase (MAPK); Phospho-p44/p42 MAPK; Nerve Growth Factor (NGF)

Introduction

Prostate cancer (PCa) is the second most common form of cancer among men worldwide [1], and a typical feature of this disease is its ability to metastasize to bone. Unremitting bone pain due to advanced metastatic spread of PCa cells to the skeleton in patients is often inadequately alleviated with current analgesics [2]. Hence, there is an unmet clinical need for novel analgesics that are efficacious and well tolerated for the relief of intractable cancer-induced bone pain [3].

To date, a large number of prohyperalgesic mediators that are released by osteoclasts, osteoblasts, tumor cells and associated immune cells have been implicated in the sensitization of peripheral components of the somatosensory system in cancer-induced bone pain [4,5]. These prohyperalgesic mediators include prostaglandins, endothelins, bradykinin, colony-stimulating factors, tumor necrosis factor-α, transforming growth factor-β, platelet-derived growth factor, interleukin-1, and interleukin-6 [5–7].

Interestingly, many peptides and peptide families that were first isolated outside the nervous system and named on the basis of a non-nociceptive physiological action have since been identified in neurons and shown to play important roles in nociception. In the latter context, they have offered new therapeutic avenues for analgesic drug discovery at a time when reliance upon opioids as the principal "strong analgesic" for cancer-related and other pains is diminishing. Apart from endothelins and bradykinin already mentioned as prohyperalgesic mediators in cancer-induced bone pain, other examples include calcitonin gene-related peptide (CGRP), substance P (Sub P), cholecystokinin [7], and now angiotensin II (Ang II) [8,9].

Although Ang II signaling via the Ang II type 1 receptor (AT_1R) is well known for its role in the regulation of blood pressure [10], Ang II signaling via the Ang II type 2 receptor (AT_2R) does not modulate blood pressure in vivo, and its physiological role has remained enigmatic [10]. However, the safety of PD123319 (also called EMA200) administered by brief (5 minutes) infusion at 10 μg/kg in 16 healthy human subjects has been evaluated in a randomized, double-blind, placebo-controlled crossover study [10]. Overall, PD123319 at the dose administered was well tolerated, and measures of cardiovascular function including blood pressure, mean arterial pressure, cardiac index, systemic vascular resistance index, reflective index and arterial stiffness index were not significantly altered relative to placebo [10].

Recent work using molecular biological (Western blot) methods in adult mice showed that the AT_2R is expressed in the brain and viscera [11], whereas in fetal mice, AT_2R expression levels were low with the exception of the skin [11]. This latter observation contrasts with earlier work by others that reported extensive AT_2R expression in the fetal rat [11]. However, after re-examination of the published autoradiographic images, Yu and colleagues concluded that AT_2R binding in the fetal rat was primarily in the skin in agreement with their more recent findings [11]. In adult rats and humans, the AT_2R is expressed on small-to–medium-sized dorsal root ganglion (DRG) neurons [12] as well as on nerve fibers in human peripheral nerves and in a range of human tissue sections including skin, urinary bladder and bowel [12].

Work from our laboratory together with that by others shows that augmented DRG levels of Ang II, the main endogenous ligand of the AT_2R, signaling via the AT_2R appear to contribute to hyperexcitability and abnormal sprouting of DRG sensory neurons in persistent pain states [8,12]. Specifically, in cultured adult rat and human DRG neurons, Ang II increased capsaicin-induced neuronal excitability and induced neurite outgrowth [12]. Both effects were attenuated in a concentration-dependent manner by EMA401 [12], an orally active small molecule AT_2R antagonist with >10,000-fold selectivity over the AT_1R [9]. Additionally, several small molecule AT_2R antagonists with >1,000-fold selectivity over the AT_1R have been shown by our laboratory to produce dose-dependent analgesia in the chronic constriction injury (CCI) of the sciatic nerve rat model of neuropathic pain [9], with analgesia abolished in CCI mice by genetic deletion of the AT_2R [8]. Ex vivo investigation of the mode of action showed that it involved blockade of augmented Ang II signaling via the AT_2R in the lumbar DRGs of CCI rats to inhibit p38 mitogen-activated protein kinase (MAPK) and p44/p42 MAPK activation [8].

Of interest herein, Jimenez-Andrade and colleagues reported that augmented nerve growth factor (NGF) signaling via its high-affinity receptor, tyrosine kinase A receptor (TrkA), has a key role in the pathobiology of PCa-induced bone pain (PCIBP) [13]. The mechanism appears to involve PCIBP-induced augmentation of NGF/TrkA signaling to induce abnormal sprouting and hyperexcitability of sensory nerve fibers in the periosteum of cancer-invaded bone [13]. In support of this notion, an NGF sequestering antibody produced analgesia in a murine model of PCIBP [14,15]. Additionally, retrograde transport of NGF from tumor-associated stromal cells [13] and/or Schwann cells [16] contributes to sensory neuron hyperexcitability via multiple mechanisms [17]. Such mechanisms include upregulated synthesis of pro-nociceptive mediators [17], activation of p38 MAPK and p44/p42 MAPK-induced [18,19] phosphorylation of the transient receptor potential vanilloid 1 (TRPV1) [19], as well as various voltage-gated sodium [20,21] and calcium ion-channels [22] implicated in the pathobiology of chronic pain [23].

Hence, the present study was designed to assess the analgesic efficacy of a small molecule AT_2R antagonist, EMA200 (also called PD123319), in a rat model of PCIBP [3] and to investigate its analgesic mode of action. Here, we show for the first time that EMA200 produced dose-dependent relief of mechanical and thermal (noxious heat) hypersensitivity in both hindpaws of a rat model of PCIBP. The mechanism involves attenuation of augmented Ang II levels in the lumbar DRGs, thus reducing augmented Ang II/AT_2R signaling that in turn reduced augmented NGF

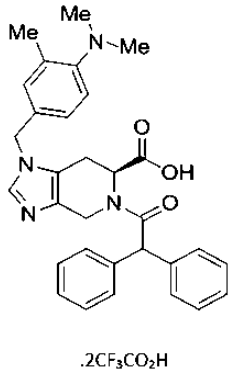

Figure 1 Chemical structure of EMA200 (also known as PD123319) ditrifluoroacetate, a small molecule angiotensin II type 2 receptor antagonist with >1,000-fold selectivity over the angiotensin II type 1 receptor [9].

signaling via TrkA, a mechanism that rapidly increases membrane expression of TRPV1 in sensory neurons [24]. The net result is inhibition of p38 MAPK and p44/p42 MAPK activation in the lumbar DRGs, key enzymes in the phosphorylation of multiple ion-channels implicated in the pathobiology of chronic pain [25,26].

Materials and Methods

Drugs and Reagents

EMA200 (also known as PD123319) ditrifluoroacetate (Figure 1) was purchased from Tocris Biosciences (Bristol, UK). Topical antibiotic powder was purchased from Apex Laboratories Pty Ltd (Somersby, NSW, Australia). Pentobarbitone sodium (Lethabarb®) was purchased from Virbac (Australia) Pty Ltd (Regents Park, NSW, Australia). Medical grade O_2 and CO_2 were purchased from BOC Gases Australia Ltd (Albion, QLD, Australia).

Animals

All procedures utilized herein were approved by the Animal Ethics Committee of The University of Queensland (Brisbane, QLD, Australia). Additionally, our experiments adhered to the *Australian Code of Practice for the Care and Use of Animals for Scientific Purposes* (7th edition, 2004). Male Wistar Han (HsdBrlHan:WIST) rats were purchased from Monash Animal Services (Melbourne, VIC, Australia) and used for experimentation herein. Rats were housed in groups of three in a temperature-controlled room (21 ± 2°C) with a 12-/12-hour light-dark cycle. Standard rodent chow and water were available *ad libitum*. Rats were acclimatized for at least 2–3 days prior to initiation of any experimentation.

Surgical Procedure

The rat AT3B PCa cells (APCCs) were purchased from the American Type Culture Collection (Manassas, VA, USA). As previously described [3], these cells were cultured, passaged (passage number 96–101), harvested, and prepared in a final concentration of 4×10^4 APCCs/10 μL phosphate-buffered saline (PBS) for unilateral intratibial injection (ITI) in rats. For preparing heat-killed cells (HKCs; sham group), APCCs were prepared in the same final concentrations and heated for 15 minutes at 85°C.

The unilateral ITI procedure was performed as previously described by our laboratory [3]. Briefly, while groups of male Wistar Han rats (90–130 g) were deeply anesthetized with 3% isoflurane delivered in oxygen, a unilateral rostrocaudal incision was made in the leg. The tibia was exposed and pierced using a 23-gauge needle, and 4×10^4 APCCs or HKCs (sham group) in a volume of 10 μL were injected into the medullary cavity using a Hamilton syringe. The bone opening was then sealed using bone wax (Ethicon, Somerville, NJ, USA), the wound was sutured, and the animals were kept warm and monitored closely during surgical recovery.

Following recovery, rats were housed in individual cages, and their general health and body weights were assessed every day throughout the experimental period. The hindpaw on the injected side is referred to as the "ipsilateral" hindpaw and the noninjected side as the "contralateral" hindpaw. All experiments were conducted during the light phase.

Behavioral Studies

Hypersensitivity (Pain) Behaviors

The temporal development of mechanical and thermal (noxious heat) hypersensitivity in the hindpaws of rats was determined using calibrated von Frey filaments (Stoelting Co., Wood Vale, IL, USA) and the Hargreaves apparatus (Ugo Basile, Comerio, VA, Italy), respectively. Briefly, von Frey filaments were used to determine the lowest mechanical threshold to elicit a paw withdrawal response (paw withdrawal threshold; PWT) in each of the hindpaws [27]. The Hargreaves apparatus was used to determine the paw thermal thresholds (PTTs) as the time to withdraw each of the ipsilateral and contralateral hindpaws in response to application of noxious heat stimuli [28].

Test Compound Administration

Solutions of the test compound in the desired concentrations (dissolved in water for injection) were prepared by one person and were assigned codes independently by a second person. For von Frey testing, where there were equal numbers of animals per group on a given day, animals were randomized by the second person. The coded test compound solutions were administered to rats by the first person, and testing was undertaken in a blinded manner. For the Hargreaves test, where the number of animals per group varied on a given day, animals were both randomized and dosed by the second person and the first person then carried out testing in a blinded manner. Each rat received up to three intravenous

(i.v.) bolus doses of EMA200 or vehicle according to a "3-day washout" protocol such that there were at least 3 days between successive doses.

Analgesic Efficacy of EMA200 at 14–21 days post-ITI. PCIBP rats with bilateral mechanical hypersensitivity secondary to a unilateral ITI of APCCs at 4×10^4 (at 14–21 days post-ITI), received single i.v. bolus doses of EMA200 (0.3, 1, and 3 mg/kg; N = 8 per dose) or vehicle. PWTs were assessed in the bilateral hindpaws immediately predose and at 0.25, 0.5, 0.75, 1.0, 1.25, 1.5, 2, and 3 hours post-dosing. Similarly, separate groups of PCIBP rats with bilateral thermal (heat) hypersensitivity were administered single i.v. bolus doses of EMA200 (1, 3, and 10 mg/kg; N = 4–7 per dose) or vehicle. Bilateral PTTs were assessed immediately predose and at 0.5, 1.0, 1.5, 2, and 3 hours post-dosing.

Behavioral Data Analyses

The pharmacological data are presented as mean (±standard error of the mean [SEM]) PWT or PTT vs time curves that were generated using the GraphPad Prism™ (v5.03) software package (GraphPad Software, Inc., San Diego, CA, USA). For PCIBP rats that received single i.v. bolus doses of EMA200 or vehicle, the PWT or PTT values are presented as differences from their baselines (ΔPWT or ΔPTT).

The extent and duration of analgesia (area under the ΔPWT vs time curves [ΔPWT AUC] and area under the ΔPTT vs time curves [ΔPTT AUC]) for EMA200 or vehicle in individual rats were determined using trapezoidal integration, and these values were normalized to the percentage of the maximum possible ΔPWT AUC (%MAX ΔPWT AUC) and ΔPTT AUC (%MAX ΔPTT AUC) values. Dose-response curves were generated by plotting mean (±SEM) %MAX ΔPWT AUC or %MAX ΔPTT AUC values vs log dose. Nonlinear regression (GraphPad Prism v5.03) was used to estimate effective dose 50% (ED_{50}) values for the relief of each of mechanical and thermal hypersensitivity in each of the ipsilateral (ED_{50IPSI}) and contralateral ($ED_{50CONTRA}$) hindpaws.

Immunohistochemistry

Tissue Collection and Preparation

Groups of drug-naïve APCC-injected (N = 6) and HKC-injected rats (N = 6) were euthanized with an overdose of pentobarbitone (1 mL/kg of 325 mg/mL Lethabarb®; Virbac Australia Pty Ltd) at 2–3 weeks post-ITI. A separate group of APCC-injected rats (N = 5) were administered EMA200 (3 mg/kg i.v.) at 14–21 days post-ITI and euthanized at the time of peak effect (0.5 hours post-dosing). After euthanasia, rats were immediately perfused transcardially with 4% paraformaldehyde (PFA). The lumbar L4-L6 DRGs were removed, post-fixed in 4% PFA for 2 hours, transferred to a 15% sucrose/PBS solution followed by a 30% sucrose/PBS solution and then a 1:1 mixture of 30% sucrose/PBS and Tissue-Tek® optimum cutting temperature (OCT) solution (Proscitech, Thuringowa, QLD, Australia), respectively, and left overnight at 4°C. Subsequently, the tissues were embedded in OCT embedding medium and stored at –80°C until used. Frozen DRG sections (10–12 μm) were cut using a cryostat (Hyrax C60 cryostat) and mounted onto Superfrost® Plus slides (Lomb Scientific, Taren Point, NSW, Australia).

Immunostaining and Image Analysis

The lumbar L4-L6 DRG tissue sections were washed with 1X PBS (pH 7.4) containing 0.3% Tween 20 (PBST) (Sigma-Aldrich, Castle Hill, NSW, Australia) solution (2 × 10 minutes), preincubated with 0.3% hydrogen peroxide (Sigma-Aldrich) in methanol for 30 minutes at room temperature, followed by incubation with 5% bovine serum albumin (BSA) in PBST (Sigma-Aldrich) for 1 hour at room temperature. Sections were then incubated overnight at 4°C with specific primary antibodies (diluted in 3% BSA/PBST) against the AT_2R (Rabbit polyclonal [ab19134] [8], 1:250, Abcam, Cambridge, MA, USA), Ang II (guinea pig polyclonal; 1:500, Bachem, Bubendorf, Switzerland), TrkA (Goat Polyclonal, 1:10, R&D Systems Inc, Minneapolis, MN, USA), NGF (Sheep polyclonal, 1:100, Abcam), phospho-p38 MAPK (pp38 MAPK) (mouse monoclonal; 1:100, Cell Signaling Technology, Inc., Danvers, MA, USA), phospho-p44/p42 MAPK (pp44/pp42 MAPK) (mouse monoclonal; 1:100, Cell Signaling Technology), neuronal nuclei (NeuN) (Mouse monoclonal, clone A60, 1:100, Millipore, Kilsyth, VIC, Australia), Sub P (Mouse monoclonal, 1:1,000, Abcam), and neurofilament 200 kDa (NF200) (Mouse monoclonal, 1:100, Abcam). The following day, the sections were washed using PBST (2 × 10 minutes) and incubated with the appropriate secondary antibody (diluted in 1.5% BSA/PBST) for 2 hours at room temperature in the dark. Secondary antibodies used were Alexa Fluor® 488 goat anti-rabbit immunoglobulin G (IgG) (H + L) (1:5,000, Invitrogen, Mount Waverley, VIC, Australia), Alexa Fluor 546 goat anti-guinea pig IgG (H + L) (1:1,000, Invitrogen), Alexa Fluor 546 donkey anti-goat IgG (H + L) (1:1,000, Invitrogen), Alexa Fluor 633 donkey anti-sheep IgG (H + L) (1:1,000, Invitrogen), and Alexa Fluor 546 goat anti-mouse IgG (H + L) (1:1,000, Invitrogen). The sections were then washed using PBST (2 × 10 minutes) and incubated with 0.1% Sudan Black B (Sigma-Aldrich) in 70% ethanol solution for 5 minutes. After subsequent washes using PBST (2 × 10 minutes), the sections were cover-slipped with ProLong® Gold anti-fade reagent with 4',6-Diamidino-2-Phenylindole, Dihydrochloride (DAPI) (Invitrogen).

All immunostained sections cover-slipped with ProLong Gold were allowed to dry at room temperature for 12 hours prior to imaging. Sections were visualized using an Axioskop 40 microscope (Carl Zeiss, Gottingen, Germany) and images of lumbar DRG sections from at least three to four different rats per group were acquired using an Axiocam MRm camera (Carl Zeiss) using the auto-exposure settings in the Axiovision Rel. v4.8 software (Carl Zeiss) [29]. There was an absence of fluorescence in negative controls where the primary antibody was omitted. To ensure that DAPI staining did not potentially obscure the

fluorescence intensity of the fluorophore of interest [30], both the single channel/fluorophore and fluorophore with DAPI images were captured separately. After imaging by the first person, all single channel/fluorophore images were randomly assigned codes by a second person and were analyzed quantitatively by the first person in a blinded manner using Axiovision Rel. v4.8 software.

The degree of immunofluorescence (IF) (densitometric count, pixels^2) and exposure time (millisecond) for each image acquired was noted. Additionally, an outline of the DRG was drawn for each image to calculate the area (μm^2) for which fluorescence intensity was measured. The degree of IF was normalized per unit area and per unit exposure time [30] for each image acquired, and fluorescence intensity was calculated as follows:

$$\text{Fluorescence intensity of section A (pixel}^2/\mu m^2/\text{ms)} = \frac{\text{(Degree of immunofluorescence of section A [pixel}^2\text{]/Area [}\mu m^2\text{])}}{\text{Exposure time of section A (millisecond)}} \quad (1)$$

The results are presented as the fold change in fluorescence intensity (pixels^2/μm^2/ms) for lumbar DRG sections from APCC-injected rats relative to the respective ipsilateral lumbar DRG sections from sham-control rats (HKC-injected group). By applying this method that takes into account both density and intensity of fluorophore, experimenter bias in data acquisition and analysis is minimized [30].

Immunocytochemistry

The APCCs were cultured on sterilized coverslips in six-well cell culture plates until they were 50–70% confluent. The cells were fixed with ice-cold acetone, washed using PBST (2 × 5 minutes) and blocked with 5% BSA in PBST for 30 minutes at room temperature. Next, cells were immunostained with primary antibodies against the AT_2R, Ang II, TrkA, NGF, pp38 MAPK, and pp44/pp42 MAPK (for 1 hour at room temperature using the dilutions described in the preceding section) and appropriate secondary antibodies (for 30 minutes at room temperature in the dark) (as described in the preceding section). Finally, the coverslips were carefully removed from the wells and were mounted onto Superfrost Plus slides with a drop of ProLong Gold antifade reagent with DAPI, such that the APCCs were against the slide surface. Subsequently, the sections were visualized using an Axioskop 40 microscope (Carl Zeiss) and were analyzed for the presence or absence of IF.

Quantitative Real-Time Polymerase Chain Reaction Analysis of AT_2R Messenger RNA Levels in Lumbar L4-L6 DRGs

Separate groups of drug-naïve APCC-injected rats with bilateral hindpaw hypersensitivity (N = 4) or HKC-injected sham controls (N = 4) were euthanized at 2–3 weeks post-ITI with an overdose of pentobarbitone. Immediately, the lumbar L4-L6 DRGs and adrenal glands were dissected and incubated in RNA*later*® solution (Ambion, Austin, TX, USA).

Subsequently, total RNA was isolated from the collected tissues using RNeasy mini kits (Qiagen Pty Ltd, Chadstone Centre, VIC, Australia) and stored at –80°C until use. The complimentary DNA (cDNA) was reverse-transcribed from total RNA using the high-capacity RNA-to-cDNA kit (Applied Biosystems, Mulgrave, VIC, Australia). The AT_2R messenger RNA (mRNA) levels were analyzed using the TaqMan® gene expression assay (Assay ID: Rn00560677_s1, Applied Biosystems). A master mix was prepared containing TaqMan Universal PCR Master Mix (5 μL), the desired TaqMan gene expression assay (0.5 μL), and distilled DNase/RNase-free distilled water (2.5 μL). Individual reactions (10 μL) contained the master mix (8 μL) and the reverse-transcribed cDNA (2 μL of reverse transcription reaction). Detection was performed on the ABI-7900HT RT-PCR System. Briefly, samples were incubated at 50°C for 2 minutes, heated to 95°C for 10 minutes, and cycled at 95°C for 15 seconds and 60°C for 1 minute for a total of 40 cycles. Analyses was performed using the ABI 7900-HT System Sequence Detection software (v2.2.1) to determine threshold cycle (C_T) values for the AT_2R (target gene) and glyceraldehyde 3-phosphate dehydrogenase (GAPD) (reference gene) in each of the samples assessed in triplicate for each of two individual experiments. Expression levels of AT_2R mRNA were normalized relative to rat GAPD expression and quantified using the delta C_T method (ΔC_T) as described as follows:

$$\frac{AT_2R\ \text{gene}}{GAPD\ \text{gene}} = \frac{(E_{GAPD})^{C_T GAPD}}{(E_{AT_2R})^{C_T AT_2R}} \quad (2)$$

where, E_{GAPD} = the amplification efficiency of the GAPD Taqman probe (1.92) and E_{AT_2R} = the amplification efficiency of the AT_2R Taqman probe (2.09). The aforementioned amplification efficiencies were determined during preliminary optimization experiments.

Western Blotting: in vitro and ex vivo

Groups of drug-naïve PCIBP rats with bilateral hindpaw hypersensitivity (N = 4) or HKC-injected sham controls (N = 3) were euthanized with an overdose of pentobarbitone. A separate group of PCIBP rats (N = 4) that received a bolus dose of EMA200 at 3 mg/kg i.v. were euthanized at the time of peak analgesic effect (0.5 hours post-dosing). After euthanasia, lumbar L4-L6 DRGs were collected immediately and stored at 4°C overnight in Allprotect Tissue Reagent (Qiagen Pty Ltd). On the following day, protein was extracted from the lumbar DRGs as well as separately cultured APCCs by sonicating in Radioimmunoprecipitation assay (RIPA) buffer (150 mM NaCl, 1% Triton X-100, 0.5% sodium deoxycholate, 0.1% sodium dodecyl sulfate, 50 mM Tris, and 1 mM Ethylenediaminetetraacetic acid (EDTA) in MilliQ water) containing protease (cOmplete ULTRA Tablets, EASYpack, Roche, Dee Why, NSW, Australia) and phosphatase inhibitors (PhosSTOP, Roche). Protein

concentrations were determined using the Pierce® BCA protein assay kit (Pierce, Rockford, IL, USA).

For Western blot analysis, 30 μg of protein was loaded on Tris-glycine precast gels (4–20% gradient) (NuSep, Homebush, NSW, Australia). Each gel was transferred to a 0.2 μm Immuno-Blot™ Polyvinylidene fluoride (PVDF) membrane (Biorad, Hercules, CA, USA), blocked in 5% BSA/Tris-buffered saline/0.1% Tween-20 (TBST), and incubated overnight at 4°C with primary antibodies (diluted in 5% BSA-TBST) against pp38 MAPK (1:500, Rabbit monoclonal, Cell Signaling Technology, Inc.), pp44/pp42 MAPK (1:500, Rabbit monoclonal, Cell Signaling Technology, Inc.), total p38 MAPK (1:500, Rabbit monoclonal, Cell Signaling Technology, Inc.), and total p44/p42 MAPK (1:2,000, Rabbit monoclonal, Cell Signaling Technology, Inc.). β-actin expression within the protein sample (1:2,000, Rabbit polyclonal, Abcam) was used as a loading control. The membranes were subsequently washed using TBST (3 × 5 minutes) and incubated at room temperature for 1 hour (in the dark) with Alexa Fluor 680 goat anti-rabbit IgG (1:1,000, Invitrogen) secondary antibody (diluted in 3% BSA-TBST). Next, after 3 × 5-minute washes using TBST, the membranes were visualized, and the resulting immunoreactivity on membranes was captured using a Li-Cor Odyssey scanner (Li-Cor, Lincoln, NE, USA). ImageJ (National Institutes of Health, Bethesda, MD, USA) was used for semiquantitative densitometric analysis to assess the expression levels of pp38 MAPK and pp44/pp42 MAPK, relative to β-actin as follows:

$$\text{Adjusted density of pp38 MAPK or pp44/pp42 MAPK of sample A} = \frac{\text{Density of pp38 MAPK or pp44/pp42 MAPK of sample A}}{\text{Density of β-actin of sample A}} \quad (3)$$

Statistical Analyses

The one-way analysis of variance (ANOVA) followed by the Newman–Keuls test was used to compare between-group differences in immunohistochemical, Western blot, and quantitative real-time polymerase chain reaction (qRT-PCR) data. Statistical analyses were performed using the GraphPad Prism v5.03 program (GraphPad Software, Inc.), and the statistical significance criterion was $P < 0.05$. For statistical comparisons using one-way ANOVA, F values together with their associated degrees of freedom are expressed as $F_{(\text{df of treatment, residual})}$.

Results

Temporal Development of Hypersensitivity (Pain) Behaviors in the Hindpaws and General Animal Health

Following unilateral ITI of 4×10^4 APCCs in male Wistar Han rats herein, there was temporal development of significant ($P < 0.05$) mechanical and thermal (noxious heat) hypersensitivity in the bilateral hindpaws at 14–21 days. By contrast, rats administered a unilateral ITI of HKCs did not develop significant ($P > 0.05$) mechanical or thermal hypersensitivity in the hindpaws for at least 21 days after ITI [3]. Importantly, there were no significant differences in the mean body weights of APCC-injected rats relative to sham rats that received a unilateral ITI of HKCs. Our findings of temporal development of hindpaw hypersensitivity and mean body weight increases agree with our previous findings (refer to Figures 2 and 4 in reference Muralidharan et al. [3]).

Increased Ang II Expression Levels in the Lumbar L4-L6 DRGs in PCIBP Rats

At 14–21 days post-ITI, there was a significant increase in the mean (±SEM) levels of Ang II-IF ($F_{(2,23)} = 14.24$, $P < 0.05$) in both the ipsilateral (~6.5- to 7.0-fold) (Figure 2D) and contralateral (~3.5- to 4.0-fold) (Figure 2E) lumbar L4-L6 DRGs of rats that received a unilateral ITI of 4×10^4 APCCs when compared with Ang II-IF levels in the ipsilateral lumbar DRGs from HKC-injected sham rats (Figure 2F). In PCIBP rats, the mean Ang II-IF levels in the ipsilateral lumbar DRGs of PCIBP rats were significantly ($P < 0.05$) higher (~1.5- to 2-fold) than the corresponding levels in the contralateral lumbar DRGs. This observation is aligned with the greater extent of hypersensitivity in the ipsilateral compared with the contralateral hindpaws in PCIBP rats. By contrast, there were no significant changes ($P > 0.05$) in the mean levels of AT_2R-IF or AT_2R mRNA in the bilateral lumbar DRGs of PCIBP rats, c.f. the ipsilateral lumbar DRGs of sham rats when assessed using both immunohistochemistry (Figure 2A–C) and qRT-PCR (Figure 2H) methods.

The specificity of the Abcam AT_2R antibody (ab19134) used for experimentation herein was previously confirmed by our laboratory, such that AT_2R-IF observed in sections of adrenal gland and lumbar DRGs of wild-type female mice was abolished in the corresponding sections from female AT_2R knockout mice [8]. The mean (±SEM) IF levels for Ang II and the AT_2R, as well as AT_2R mRNA levels in the lumbar DRGs of PCIBP rats, relative to the corresponding levels in the ipsilateral lumbar DRGs of HKC-injected sham-rats, are summarized in Figure 2G,H.

Co-Localization of AT_2R/Ang II with Sensory Neuron Markers in Rat Lumbar DRG Sections

Specific immunofluorescently labeled antibodies show co-localization (Figure 3K–O) of the AT_2R (Figure 3A–E) with: 1) Ang II, its main endogenous ligand (Figure 3F,K); 2) Sub P, a marker of small/medium diameter nociceptive neurons (Figure 3G,L); 3) NF200, a marker of medium/large diameter nociceptive neurons (Figure 3H,M); 4) NeuN, a marker for neuronal cells (Figure 3I,N); as well as 5) NGF (Figure 3J,O) and its high affinity receptor, TrkA (in adjacent DRG sections) (Figure 3P), in the ipsilateral lumbar DRGs of PCIBP rats.

APCCs Express Ang II, AT_2R, TrkA, and pp44/pp42 MAPK but not NGF or pp38 MAPK

Using specific immunofluorescently labeled antibodies, our data show that APCCs express the AT_2R (Figure 4A),

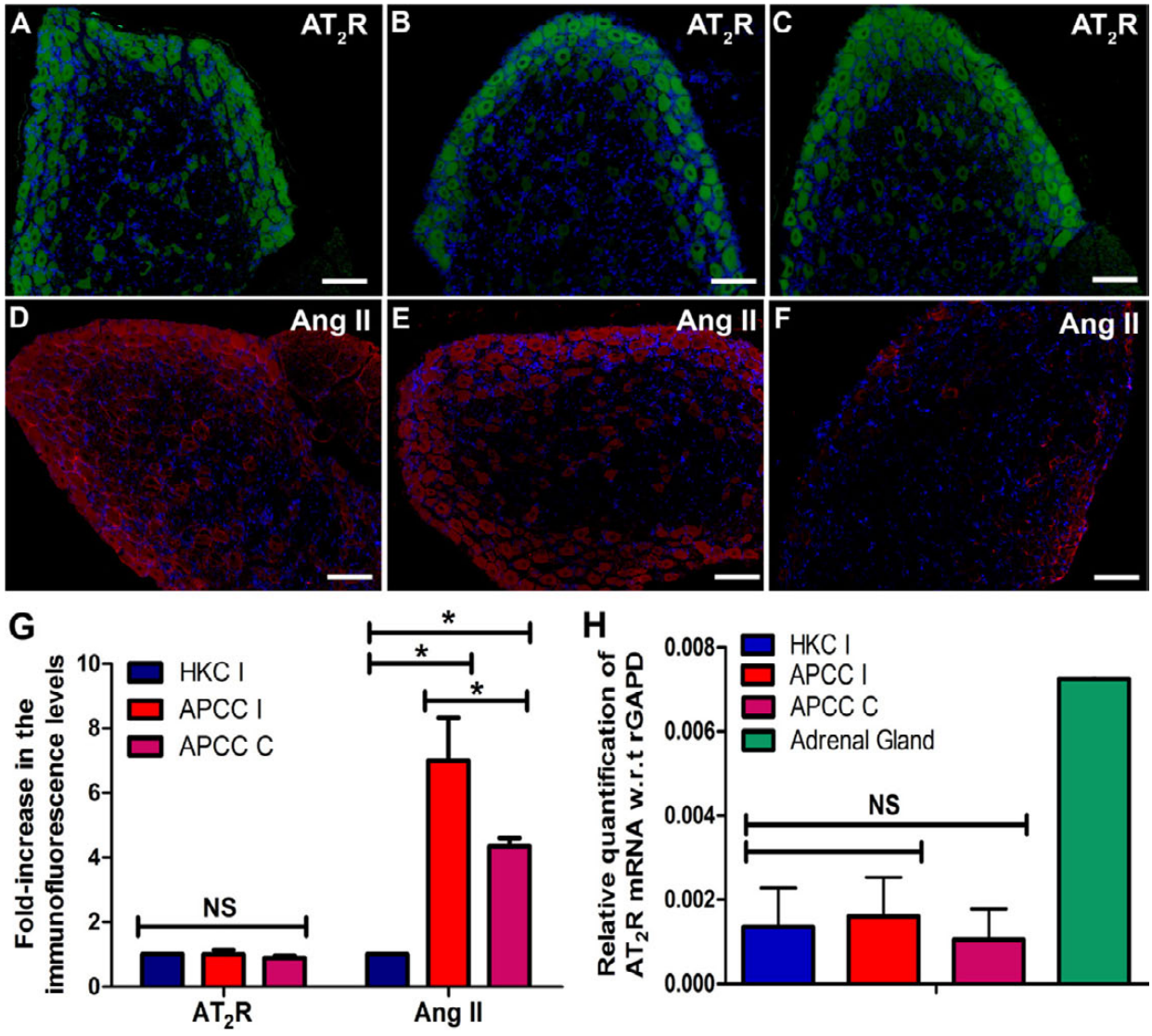

Figure 2 Augmented angiotensin II (Ang II) expression levels in the lumbar L4-L6 dorsal root ganglia (DRGs) of prostate cancer-induced bone pain (PCIBP) rats. (A–C) Ang II type 2 receptor (AT_2R) and (D–F) Ang II immunostaining in the (A and D) ipsilateral and (B and E) contralateral lumbar DRGs of PCIBP rats, relative to the (C and F) ipsilateral lumbar DRGs of heat-killed cell (HKC)-injected rats at 14–21 days post-unilateral intratibial injection (ITI). The mean (±standard error of the mean [SEM]) immunofluorescence (IF) levels for Ang II were significantly higher in both the (D) ipsilateral and (E) contralateral lumbar DRGs of PCIBP rats relative to the mean Ang II-IF levels in the (F) ipsilateral lumbar DRGs of HKC-injected rats. By contrast, there were no significant changes ($P > 0.05$) in the mean levels of AT_2R-IF or AT_2R messenger RNA (mRNA) in the bilateral lumbar DRGs of PCIBP rats, cf. the ipsilateral lumbar DRGs of HKC-injected rats. (G and H) Between-group comparison of the mean (±SEM) levels of (G) Ang II- and AT_2R-IF, and (H) AT_2R mRNA levels in the lumbar DRGs at 2–3 weeks post-unilateral ITI of AT3B prostate cancer cell (APCCs) or HKCs (sham group) in Wistar Han rats. $^{*}P < 0.05$; $^{NS}P > 0.05$. Scale bar: 50 μm.

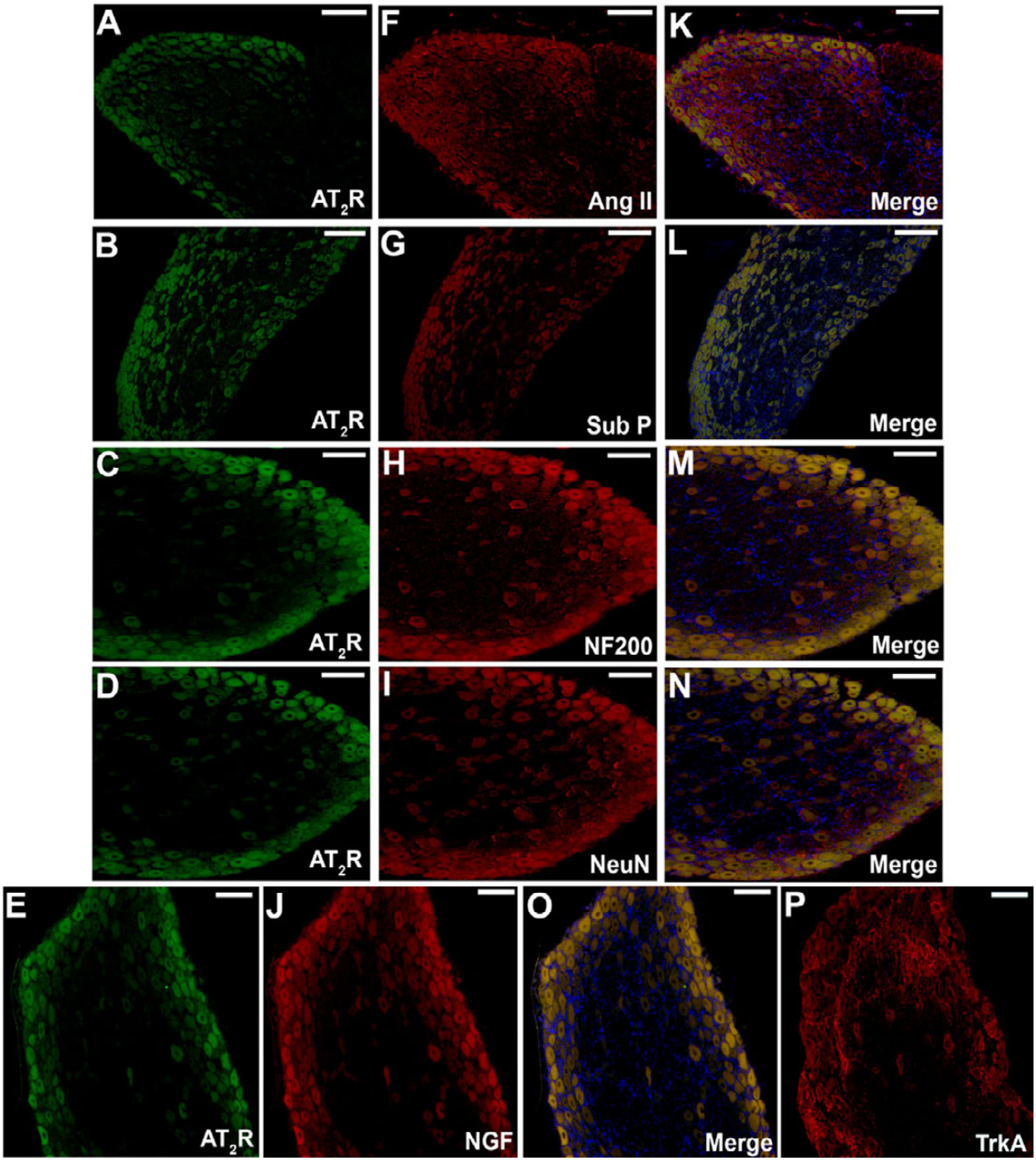

Figure 3 Immunostaining of sections of ipsilateral lumbar L4-L6 dorsal root ganglia (DRGs) from prostate cancer-induced bone pain (PCIBP) rats at 14–21 days post-intratibial injection (ITI). Specific immunofluorescently labeled antibodies show that in lumbar DRG sections (A–E) the angiotensin II type 2 receptor (AT_2R) (green) and each of (F) angiotensin II (Ang II), (G) substance P (Sub P), (H) neurofilament 200 kDa (NF200), (I) neuronal nuclei (NeuN), and (J) nerve growth factor (NGF) are co-localized (K–O) (yellow). Consecutive lumbar DRG sections from PCIBP rats immunostained with a specific tyrosine kinase A (TrkA) antibody indicate likely co-localization of the (E) AT_2R and (P) TrkA. Scale bar: 50 μm.

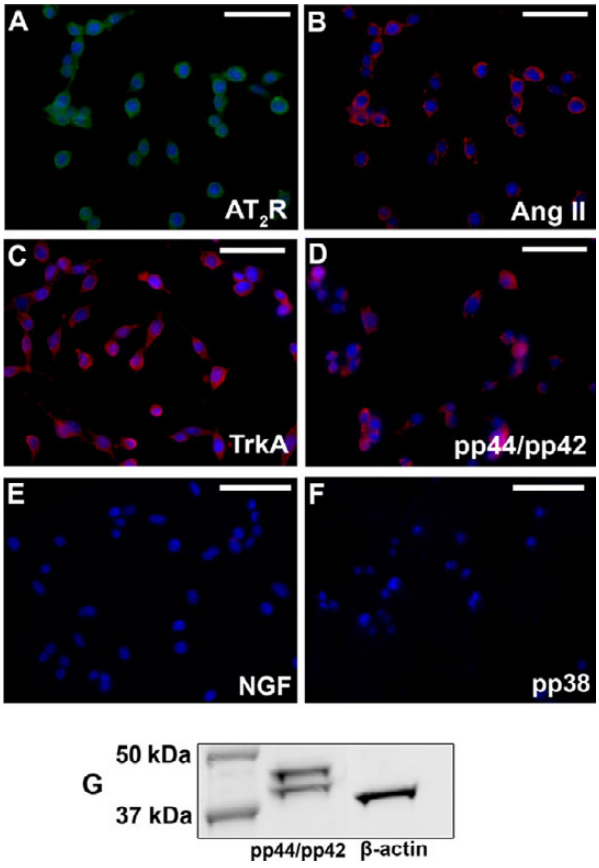

Figure 4 Immunocytochemistry of AT3B prostate cancer cells (APCCs). Specific immunofluorescently labeled antibodies show expression of the (A) angiotensin II type 2 receptor (AT_2R), (B) angiotensin II (Ang II), (C) tyrosine kinase A (TrkA), and (D) pp44/pp42 mitogen-activated protein kinase (MAPK) by APCCs. By contrast, immunofluorescence for (E) nerve growth factor (NGF) and (F) pp38 MAPK was not observed on APCCs. Western blotting was used to confirm expression of (G) pp44/pp42 MAPK by APCCs. Scale bar: 50 μm.

Ang II (Figure 4B), TrkA (Figure 4C), and pp44/pp42 MAPK (Figure 4D). By contrast, IF for NGF (Figure 4E) and pp38 MAPK (Figure 4F) was not observed on APCCs. The expression of pp44/pp42 MAPK by APCCs was also confirmed using Western blot (Figure 4G).

Analgesic Efficacy of EMA200 at 14–21 Days Post-ITI in PCIBP Rats

In PCIBP rats with bilateral mechanical hypersensitivity at 2–3 weeks post-unilateral ITI, administration of single i.v. bolus doses of EMA200 (0.3–3 mg/kg) produced dose-dependent pain relief (Figure 5A,B) in each of the ipsilateral (Figure 5A) and contralateral (Figure 5B) hindpaws, whereas vehicle was inactive. Similarly, administration of single i.v. bolus doses of EMA200 (1–10 mg/kg), but not vehicle, produced dose-dependent relief of thermal (noxious heat) hypersensitivity (Figure 5C,D) in each of the ipsilateral (Figure 5C) and contralateral (Figure 5D) hindpaws in a separate group of PCIBP rats.

After i.v. bolus dose administration of EMA200 in PCIBP rats, there was a rapid onset of action for relief of mechanical and thermal hypersensitivity in the bilateral hindpaws with mean peak analgesia observed at 0.5 hours post-dosing. At the highest dose tested, the mean duration of action for relief of mechanical hypersensitivity (3 mg/kg) and relief of thermal hypersensitivity (10 mg/kg) was ~1.5 and >3 hours, respectively. The mean (±SEM) extent and duration of pain relief (%MAX ΔPWT AUC and %MAX ΔPTT AUC) vs dose curves for EMA200 relative to vehicle for each of the ipsilateral and contralateral hindpaws are shown in Figure 5E–H. The mean (95% confidence interval [CI]) ED_{50IPSI} and $ED_{50CONTRA}$ values for the relief of mechanical hypersensitivity in the hindpaws were 0.8 (95% CI 0.61–1.03) mg/kg and 1.8 (95% CI 1.2–2.8) mg/kg, respectively. The corresponding mean ED_{50} values for the relief of thermal hypersensitivity in the ipsilateral and contralateral hindpaws were 3.9 (95% CI 3.0–5.2) mg/kg and 5.5 (95% CI 3.9–7.7) mg/kg, respectively.

Effect of EMA200 on Expression Levels of Pro-Hyperalgesic Mediators, Ang II, and the AT_2R in Lumbar L4-L6 DRGs of PCIBP Rats

pp38 MAPK and pp44/42 MAPK

For PCIBP rats with bilateral hindpaw hypersensitivity at 2–3 weeks post-unilateral ITI of APCCs, mean IF levels for pp38 MAPK ($F_{(2,23)} = 28.07$, $P < 0.05$) and pp44/pp42 MAPK ($F_{(2,24)} = 24.34$, $P < 0.05$) were significantly higher in both ipsilateral (pp38 MAPK [~10.0- to 10.5-fold] and pp44/pp42 MAPK [~8.5- to 9.0-fold]) (Figure 6B,H) and contralateral (pp38 MAPK [~5.0- to 5.5-fold] and pp44/pp42 MAPK [~4.0- to 4.5-fold]) (Figure 6C,I) lumbar DRGs, cf. the corresponding mean IF levels in the ipsilateral lumbar DRGs of sham rats (Figure 6A,G).

At the time of peak analgesia (0.5 hours post-dosing) evoked by EMA200 at 3 mg/kg i.v. in PCIBP rats, there was a significant reduction (~3.0- to 3.5-fold) in the mean ipsilateral (Figure 6D) lumbar DRG levels of pp38 MAPK ($F_{(2,28)} = 40.73$, $P < 0.05$), cf. the corresponding mean IF levels for the lumbar DRGs of drug-naïve PCIBP rats. Additionally, administration of EMA200 at 3 mg/kg i.v. to PCIBP rats significantly reduced the mean ipsilateral (Figure 6J) lumbar DRG levels of pp44/42 MAPK ($F_{(2,24)} = 43.48$, $P < 0.05$) to match the respective levels in sham controls. The significant reduction in mean IF levels for pp38 MAPK ($F_{(4,13)} = 84.21$, $P < 0.05$) and pp44/42 MAPK ($F_{(4,13)} = 112.6$, $P < 0.05$) in the lumbar DRGs of PCIBP rats at the time of peak-effect of EMA200 was confirmed using Western blot analysis (Figure 6E,K).

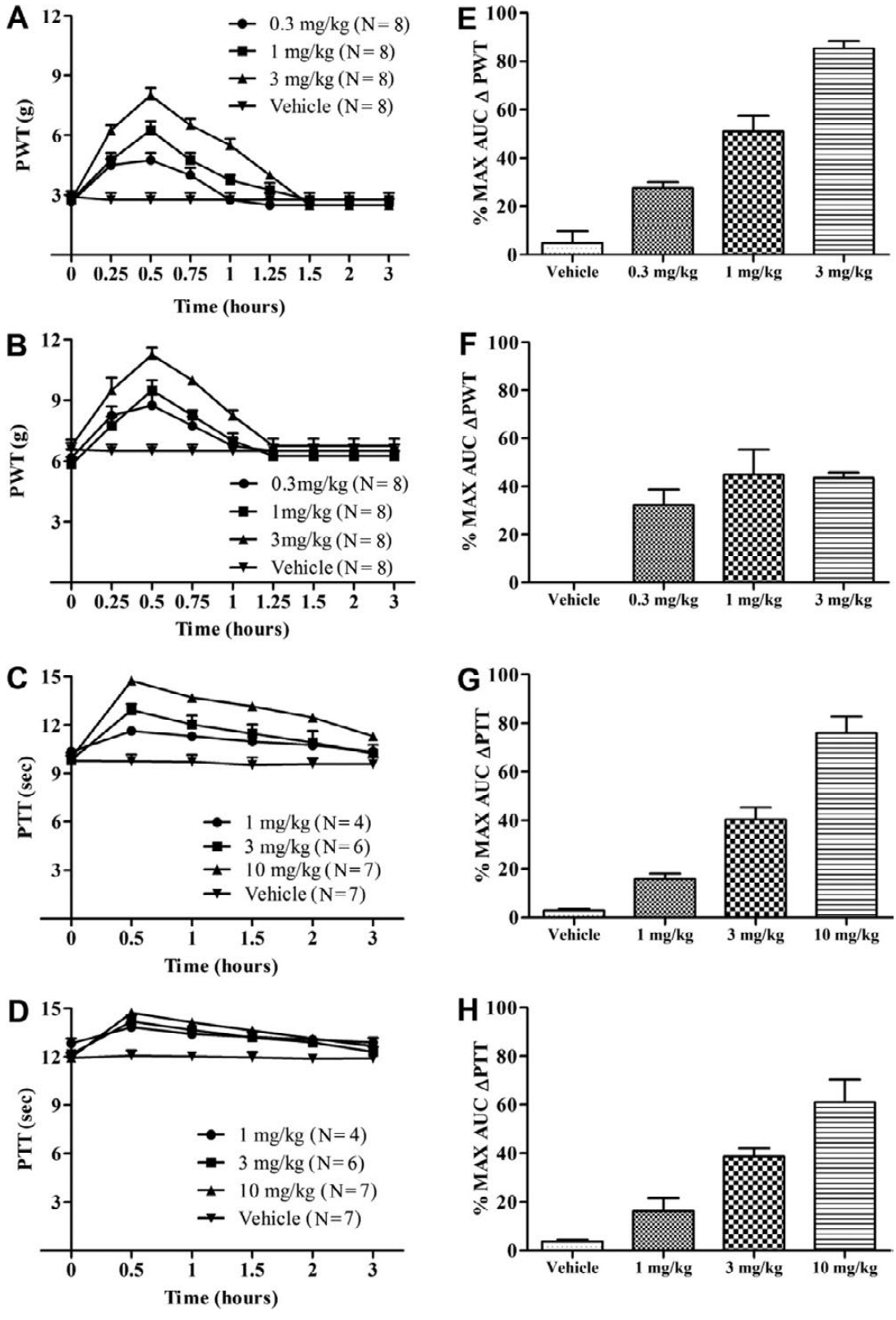

Figure 5 EMA200 evokes dose-dependent analgesia in the bilateral hindpaws of prostate cancer-induced bone pain (PCIBP) rats. Mean (±standard error of the mean [SEM]) (A and B) paw withdrawal threshold (PWT) and (C and D) paw thermal threshold (PTT) vs time curves for the (A and C) ipsilateral and (B and D) contralateral hindpaws of PCIBP rats following administration of single intravenous (i.v.) bolus doses (0.3–10 mg/kg) of the selective small molecule angiotensin II type 2 receptor (AT_2R) antagonist, EMA200, or vehicle, at 2–3 weeks post-unilateral intratibial injection (ITI). (E–H) Mean (±SEM) (E and F) %MAX ΔPWT AUC and (G and H) % MAX ΔPTT AUC values (extent and duration of analgesia) vs dose relationships for the (E and G) ipsilateral and (F and H) contralateral hindpaws of PCIBP rats following administration of single i.v. bolus doses of EMA200 or vehicle to PCIBP rats.

There were no significant ($P > 0.05$) between-group differences in the expression levels of total p38 MAPK (Figure 6F), total p44/p42 MAPK (Figure 6L), and β-actin (Figure 6M). The aforementioned relative changes in the mean (±SEM) IF and Western blot expression levels of pp38 MAPK and pp44/42 MAPK are summarized in Figure 6N–P.

NGF, TrkA, and Sub P

At 2–3 weeks post-ITI in PCIBP rats, there were significant increases in the mean IF levels for NGF ($F_{(2,24)} = 12.75$, $P < 0.05$) (ipsilateral [~3.0- to 3.5-fold] and contralateral [~2.0- to 2.5-fold]) (Figure 7D,G) and TrkA ($F_{(2,30)} = 7.41$, $P < 0.05$) (Figure 7E,H) (ipsilateral [~2.5- to 3.0-fold] and contralateral [~3.0- to 3.5-fold]) in the bilateral lumbar DRGs, relative to the corresponding mean IF levels in the ipsilateral lumbar DRGs of sham (HKC-injected) rats (Figure 7A,B for NGF and TrkA, respectively). At the time of peak analgesia of a bolus dose of EMA200 (3 mg/kg i.v.), there was a significant decrease in the mean IF levels for NGF ($F_{(2,27)} = 22.68$, $P < 0.05$) in the ipsilateral (Figure 7J) lumbar DRGs of PCIBP rats to match the respective levels in the ipsilateral lumbar DRGs of sham controls (Figure 7A).

By contrast, mean IF levels for TrkA in the ipsilateral lumbar DRGs of PCIBP rats (~2.5- to 3.0-fold) (Figure 7K) were not significantly altered ($P > 0.05$) at the time of peak EMA200 (3 mg/kg i.v.) analgesia. There were also no significant changes ($P > 0.05$) in the mean IF levels for Sub P in the bilateral lumbar DRGs of PCIBP rats (Figure 7F,I), cf. ipsilateral lumbar DRGs of HKC-injected rats (Figure 7C). Levels of IF for Sub P in the ipsilateral lumbar DRGs of PCIBP rats were not significantly altered ($P > 0.05$) at the time of peak effect of EMA200 at 3 mg/kg i.v. (Figure 7L).

The aforementioned relative changes in mean (±SEM) IF levels for NGF, TrkA, and Sub P are summarized in Figure 7M.

Ang II and the AT_2R

At the time of peak analgesia (0.5 hours post-dosing) evoked by a single i.v. bolus dose of EMA200 at 3 mg/kg in PCIBP rats, the elevated mean IF levels for Ang II were significantly reduced ~2.0- to 2.5-fold ($F_{(2,23)} = 9.27$, $P < 0.05$) in the ipsilateral lumbar DRGs (Figure 7M), cf. the Ang II-IF levels in the ipsilateral lumbar DRGs of drug-naïve PCIBP rats. Additionally, at the time of peak EMA200 analgesia in PCIBP rats, the mean ipsilateral lumbar DRG IF levels for Ang II were similar ($P > 0.05$) to the corresponding levels in the contralateral lumbar DRGs of drug-naïve PCIBP rats (Figure 7M). For the AT_2R, mean IF levels in the ipsilateral lumbar DRGs of PCIBP rats administered an i.v. bolus dose of EMA200 at 3 mg/kg did not differ significantly ($P > 0.05$) from the corresponding levels for the lumbar DRGs of drug-naïve PCIBP rats (Figure 7M).

Discussion

Here, we show for the first time that single i.v. bolus doses of the small molecule AT_2R antagonist, EMA200 that has >1,000-fold selectivity over the AT_1R [9], produced dose-dependent relief of both mechanical and thermal hypersensitivity in the bilateral hindpaws of PCIBP rats (Figure 5A–D). EMA200 analgesia in PCIBP rats was characterized by a rapid onset of action with the mean peak effect observed at approximately 0.5 hours post-dosing (Figure 5A–D).

Our present findings extend previous work from our laboratory showing that several small molecule AT_2R antagonists, viz. EMA200, EMA300, and EMA401, produced dose-dependent analgesia in the ipsilateral hindpaws of rats with a unilateral CCI of the sciatic nerve, a widely utilized rodent model of neuropathic pain [9]. In CCI-mice null for the AT_2R, EMA300 analgesia was abolished affirming that the AT_2R is essential for mediating its analgesic effects [8]. Additionally, we showed that the radioligand binding affinity of the orally active AT_2R antagonist, EMA401, for the AT_2R is similar between rats and humans [9], and that EMA401 has >10,000-fold binding selectivity for both the rat and human AT_2R vis-à-vis the AT_1R [9]. Hence, it is plausible that the analgesic effects of AT_2R antagonists in rodent models of neuropathic pain will translate to humans. In support of this notion, a recent randomized, double-blind, placebo-controlled, phase 2 clinical trial (ACTRN 12611000822987) in 183 patients administered twice-daily oral doses of the small molecule

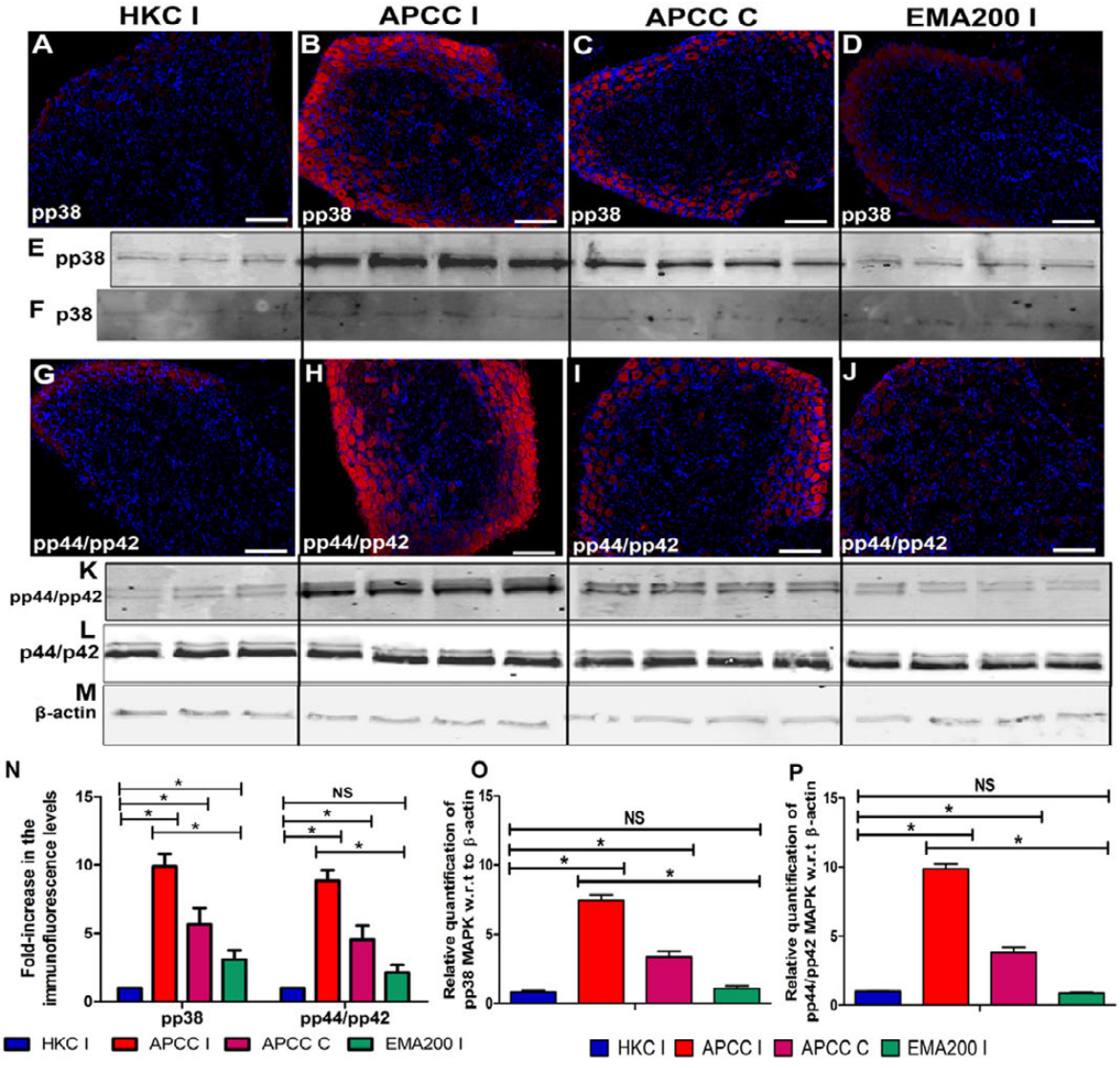

Figure 6 An analgesic dose of EMA200 inhibited p38 mitogen-activated protein kinase (MAPK) and p44/p42 MAPK activation in the lumbar L4-L6 dorsal root ganglia (DRGs) of prostate cancer-induced bone pain (PCIBP) rats. In PCIBP rats at 14–21 days post-intratibial injection (ITI), there was a significant increase ($P < 0.05$) in the mean (B and H) ipsilateral and (C and I) contralateral lumbar DRG immunofluorescence (IF) levels for pp38 MAPK and pp44/pp42 MAPK, c.f. the corresponding mean IF levels in the (A and G) ipsilateral lumbar DRGs of heat-killed cell (HKC)-injected rats. At the time of peak analgesia (0.5 hours post-dosing) of EMA200 (3 mg/kg intravenous [i.v.]), the elevated IF levels for pp38 MAPK and pp44/pp42 MAPK in the (D and J) ipsilateral lumbar DRGs of PCIBP rats were significantly reduced ($P < 0.05$) compared with the corresponding IF levels for the ipsilateral lumbar DRGs of drug-naïve PCIBP rats. For pp44/pp42 MAPK, mean IF levels were reduced ($P < 0.05$) to match the corresponding levels in the ipsilateral lumbar DRGs of HKC-injected rats. Similar relative changes in the lumbar DRG expression levels for (E) pp38 MAPK and (K) pp44/pp42 MAPK were observed using Western blot. There were no significant ($P > 0.05$) between-group differences for expression levels of (F) total p38 MAPK, (L) total p44/p42 MAPK, and (M) β-actin. (N–P) Between-group comparison of the mean (±standard error of the mean [SEM]) (N) IF levels and (O and P) Western blot expression levels of pp38 MAPK and pp44/42 MAPK in the lumbar DRGs. *$P < 0.05$. Scale bar: 50 μm.

AT_2R antagonist, EMA401 at 100 mg/kg for 4 weeks, successfully alleviated post-herpetic neuralgia, with a good safety and tolerability profile [31]. EMA401 does not cross the blood-brain barrier [12] that is consistent with its lack of central nervous system side effects [31].

Herein, we used specific immunofluorescently labeled antibodies to show co-localization of the AT_2R with Sub P and NF-200, markers of small/medium and medium/large diameter sensory neurons, respectively, in rat lumbar DRGs, in agreement with a recent report by our laboratory [8]. Our findings are consistent with work by others showing that ~50–60% of small/medium diameter human DRG neurons as well as painful human neuromas express the AT_2R [12]. Additionally, co-localization of Ang II with Sub P and NF-200 in adult rat DRG sections herein, is similar to findings reported previously by our laboratory and others in adult rat and human DRGs [8,32].

A role for augmented Ang II signaling via the AT_2R in pro-nociceptive signaling in the peripheral nervous system is supported by the fact that Ang II increases capsaicin-induced excitability of cultured adult rat and human DRG sensory neurons with this effect inhibited in a concentration-dependent manner by the small molecule AT_2R antagonist, EMA401 [12], that has 10,000-fold selectivity over the AT_1R [9]. This is of particular interest, as hyperexcitability of first-order sensory neurons contributes to the pathobiology of cancer-induced bone pain [33]. Similar changes in the excitability of primary sensory neurons underpin the development and/or maintenance of a range of difficult-to-control chronic pain states [34–36].

Ex vivo investigation of the analgesic mode of action of EMA200 in PCIBP rats exhibiting mechanical and thermal (noxious heat) hypersensitivity in the bilateral hindpaws herein shows that APCC-induced increases in mean IF levels for NGF and pp44/pp42 MAPK in the ipsilateral lumbar DRGs were significantly ($P < 0.05$) reduced to match the respective levels in the sham controls. Additionally, at the time of peak EMA200-mediated analgesia, there were significant ($P < 0.05$) decreases in the mean ipsilateral lumbar DRG IF levels of pp38 MAPK and Ang II compared with the corresponding IF levels in the ipsilateral lumbar DRGs of drug-naïve PCIBP rats. By contrast, the elevated mean IF levels for TrkA observed in the ipsilateral lumbar DRGs of PCIBP rats, c.f. the corresponding levels for sham-control rats were not significantly altered ($P > 0.05$) at the time of peak EMA200 analgesia. In the lumbar DRGs of PCIBP rats, mean levels of AT_2R mRNA as well as IF for Sub P and the AT_2R did not differ significantly ($P > 0.05$) from the corresponding levels in the ipsilateral lumbar DRGs of sham-control rats. Additionally, Sub P and AT_2R IF levels were not altered at the time of peak EMA200 analgesia in PCIBP rats.

Together, our ex vivo data suggest that single i.v. bolus doses of the AT_2R antagonist, EMA200, produce analgesia in PCIBP rats by attenuation of augmented Ang II/AT_2R signaling in the ipsilateral lumbar DRGs by both a reduction in augmented lumbar DRG levels of Ang II and blockade of the AT_2R. This attenuation of augmented Ang II/AT_2R signaling in turn reduced the marked elevation in the lumbar DRG levels of NGF in PCIBP rats to attenuate augmented NGF/TrkA signaling, with the net result being inhibition of p38 MAPK and p44/p42 MAPK activation. This latter notion is supported by previous work by others showing that administration of an NGF sequestering antibody [37] or a non-selective Trk receptor inhibitor (K252a) [38] to attenuate augmented NGF/TrkA signaling resulted in inhibition of p38 MAPK and p44/p42 MAPK activation in the lumbar DRGs of rat models of neuropathic and inflammatory pain, respectively. Blockade of p38 MAPK and p44/p42 MAPK activation in turn would be expected to reduce the activation (phosphorylation) of multiple receptors and ion channels implicated in the pathobiology of chronic pain [23], including TRPV1 and its NGF-dependent increase in neuronal membrane expression [19,24] as well as voltage-gated sodium [20,21] and calcium channels [22].

Our present findings implicating attenuation of augmented Ang II/AT_2R signaling to reduce augmented NGF/TrkA signaling to produce inhibition of p38 MAPK and p44/p42 MAPK activation in the ipsilateral lumbar DRGs in the analgesic mode of action of an AT_2R antagonist (EMA200) in PCIBP rats extend our previous findings in a rat model of neuropathic pain [8]. Specifically, we previously showed that the small molecule AT_2R antagonist, EMA300 (a structural analog of EMA200), produced analgesia in the widely utilized CCI rat model of neuropathic pain by a mechanism involving inhibition of augmented Ang II signaling via the AT_2R that in turned blocked p38 MAPK and p44/p42 MAPK activation in the ipsilateral lumbar DRGs [8]. This mode of action is consistent with work by others showing that inhibitors of p38 MAPK and p44/p42 MAPK activation produce analgesia in various rodent models of inflammatory and neuropathic pain [39–43]. Investigation of the safety and efficacy of p38 MAPK inhibitors in inflammatory disease conditions including rheumatoid arthritis, Crohn's disease, asthma ,and psoriasis over the past two decades, resulted in several clinical trials being terminated early due to toxicity (see Coulthard et al. [44] for review). However, it is now appreciated that an attractive strategy for achieving the desired efficacy while minimizing adverse events evoked by direct p38 MAPK inhibition is to develop drugs that modulate targets, such as the AT_2R herein, that regulate p38 MAPK function [44].

In cultured adult rat and human DRG neurons, Ang II signaling via the AT_2R not only augmented capsaicin-induced neuronal excitability [12], it also induced neurite outgrowth [12] in a manner similar to earlier work in cultured cells of neuronal origin (NG 108-15 and PC12W cells) [45–47]. As Ang II signalling via the AT_2R to induce neurite outgrowth in cells of neuronal origin is underpinned by sustained activation of p44/p42 MAPK [45–47], we propose that small molecule AT_2R antagonists will reduce ectopic sprouting of primary afferent sensory nerve fibers via a similar mechanism. Hence, the analgesic effects of AT_2R antagonists in the chronic dosing setting are likely to be underpinned by inhibition of

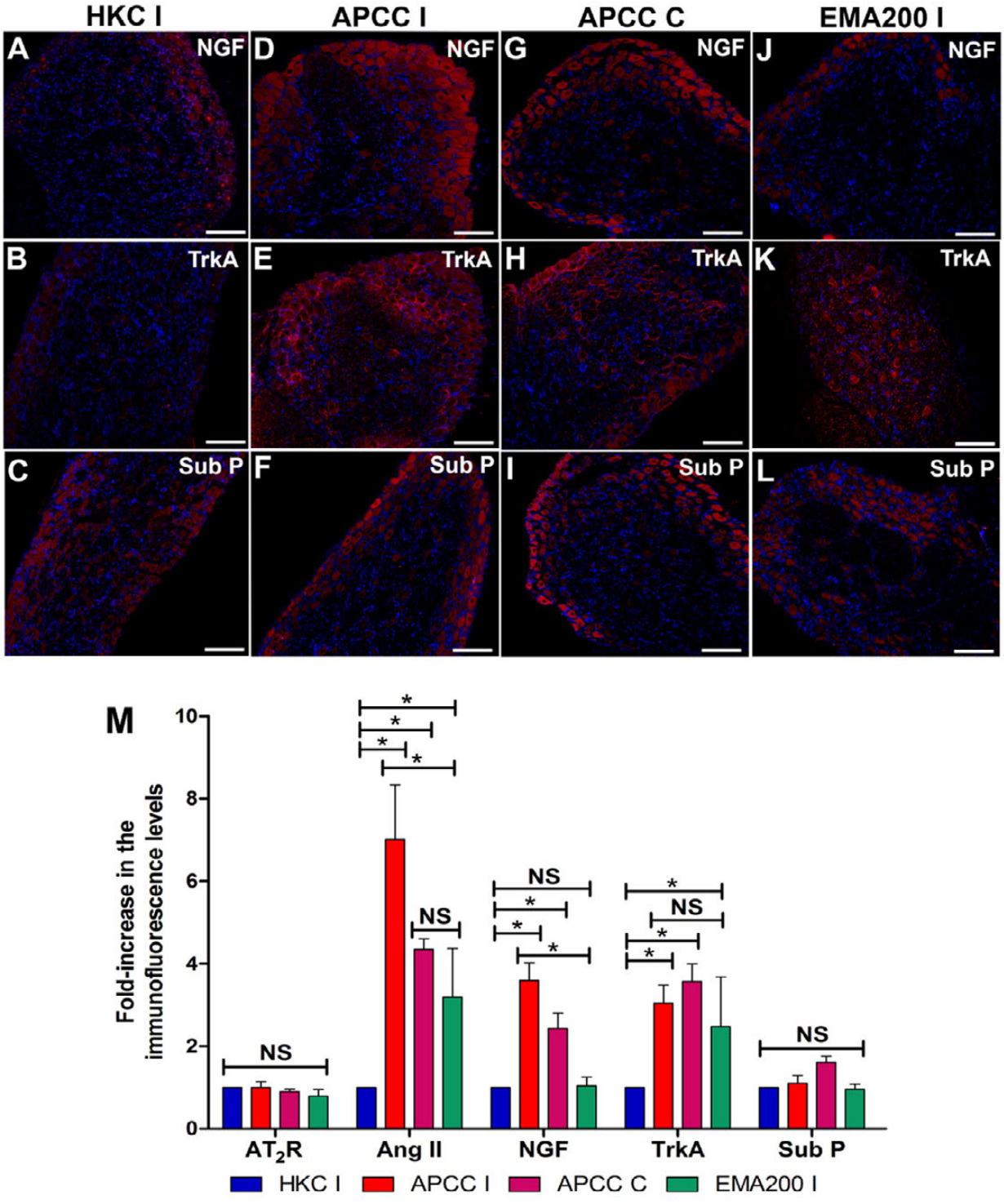

augmented Ang II/AT_2R signaling-induced DRG neuron hyperexcitability as well as inhibition of ectopic sprouting of primary afferent sensory nerve fibers; this latter notion remains for future investigation.

The broader implications of our findings that augmented Ang II signaling via the AT_2R in lumbar DRGs contributes to the pathobiology of PCIBP and neuropathic pain [8,9], and that Ang II is yet another peptide first isolated and

Figure 7 Effect of an analgesic dose of EMA200 on expression levels of angiotensin II (Ang II), Ang II type 2 receptor (AT_2R), nerve growth factor (NGF), tyrosine kinase A receptor (TrkA) and substance P (Sub P) in the lumbar L4-L6 dorsal root ganglia (DRGs) of prostate cancer-induced bone pain (PCIBP) rats. Immunostaining for (A, D, G, and J) nerve growth factor (NGF), (B, E, H, and K) TrkA, and (C, F, I, and L) Sub P in sections of (D–I) bilateral lumbar DRGs of drug-naïve PCIBP rats, (J–L) ipsilateral lumbar DRGs of PCIBP rats administered EMA200 (3 mg/kg intravenous [i.v.]), and (A–C) ipsilateral lumbar DRGs of sham-control rats, at 14–21 days post-intratibial injection (ITI). (M) Between-group comparison of the mean (±standard error of the mean [SEM]) immunofluorescence (IF) levels for the AT_2R, Ang II, NGF, TrkA, and Sub P in the bilateral lumbar DRGs of PCIBP rats compared with the ipsilateral lumbar DRGs from the sham-control rats or the ipsilateral lumbar DRGs of PCIBP rats administered EMA200 at 3 mg/kg i.v., relative to the ipsilateral lumbar DRGs of drug-naïve PCIBP rats. There was a significant ($P < 0.05$) increase in the mean IF levels for Ang II, NGF, and TrkA in each of the ipsilateral and contralateral lumbar DRGs of PCIBP rats, relative to the corresponding mean IF levels in the ipsilateral lumbar DRGs of sham (heat-killed cell [HKC]-injected) rats. At the time of peak analgesia of EMA200 at 3 mg/kg i.v. in PCIBP rats, mean IF levels for NGF in the ipsilateral lumbar DRGs were significantly ($P < 0.05$) reduced to match the respective levels in sham controls. Additionally, administration of EMA200 at 3 mg/kg to PCIBP rats significantly ($P < 0.05$) reduced the mean ipsilateral lumbar DRG IF levels of Ang II by ~2.0- to 2.5–fold, cf. the Ang II-IF levels in the ipsilateral lumbar DRGs of drug-naïve PCIBP rats. By contrast, administration of EMA200 to PCIBP rats did not significantly alter ($P > 0.05$) the mean ipsilateral lumbar DRG IF levels for TrkA. There were no significant changes ($P > 0.05$) in the IF levels for the AT_2R or Sub P in the bilateral lumbar DRGs of drug-naïve PCIBP rats or the ipsilateral lumbar DRGs of PCIBP rats administered EMA200 when compared with the corresponding IF levels in the ipsilateral lumbar DRGs of HKC-injected rats. *$P < 0.05$. Scale bar: 50 μm.

demonstrated to have a physiological role outside the nervous system, but subsequently shown to be present in neurons and to be a prohyperalgesic mediator [23]. Examples include CGRP, Sub P, bradykinin, cholecystokinin, endothelin [7,23], and now, Ang II [8,9]. Drug discovery strategies aimed at reducing their prohyperalgesic activities hold promise for analgesic drug discovery at a time when reliance upon opioids as the principal "strong analgesic" for cancer-related and other types of chronic pain is diminishing.

Over the past decade, NGF signaling via TrkA has emerged as a key factor in the sensitization of first-order sensory neurons [48] and in the ectopic sprouting/pathological remodelling of sensory nerve fibers that underpins their hyperexcitability in various difficult-to-control pain states, including cancer induced bone pain [13,16,49–51]. NGF-induced neurite outgrowth in cultured adult rat DRG neurons was reportedly unaffected by AT_2R blockade with PD123319 (EMA200) [52]. This previous observation is consistent with our present findings showing that at the time of peak effect of an analgesic dose of EMA200, the PCa bone pain-induced large increase in mean lumbar DRG NGF levels was reduced to match the corresponding levels in sham-control rats. Hence, EMA200 inhibition of augmented Ang II/AT_2R signaling appears to be upstream of the augmented NGF/TrkA signaling cascade in the DRGs. Our data together with the fact that all of the components of an intrinsic angiotensinergic system are present in bone [53] suggest that NGF-induced abnormal sprouting and hyperexcitability of TrkA-expressing sensory nerve fibers reported by others in the periosteum of PCa cell-invaded bone [13] may be regulated by augmented Ang II signaling via the AT_2R. However, this notion remains for future detailed investigation.

In a nude mouse model of PCIBP involving unilateral ITI of canine ACE-1 PCa cells, the cellular source of NGF to drive ectopic sprouting of $TrkA^+$-sensory nerve fibers was proposed as tumor-associated inflammatory and/or stromal cells as there was no detectable NGF mRNA in the canine PCa cells [13]. It is also possible that NGF synthesized by Schwann cells may contribute to axonal sprouting of sensory nerve fibers and neuroma formation in a manner similar to that for rodent models of peripheral nerve injury-induced neuropathic pain [16,51,54,55]. Here, although we found an absence of NGF IF in APCCs, our data show that APCCs do express Ang II, the AT_2R, and TrkA in agreement with others [56,57]. A role for augmented Ang II signaling via the AT_2R on APCCs to stimulate ectopic sprouting of $TrkA^+$-sensory nerve fibers in cancer-invaded bone in PCIBP rats is supported by our present finding that APCCs express pp44/pp42 MAPK. This is reminiscent of Ang II signaling via the AT_2R to

stimulate neurite outgrowth in cultured cells of neuronal origin by a mechanism involving sustained activation of p44/p42 MAPK [45].

Conclusion

In summary, we show for the first time that single i.v. bolus doses of EMA200, a small molecule AT_2R antagonist with >1,000-fold selectivity over the AT_1R, produces dose-dependent analgesia in a rat model of PCIBP. The analgesic mode of action in PCIBP rats involves inhibition of augmented Ang II signaling via the AT_2R in the lumbar DRGs to attenuate augmented NGF signaling via TrkA in the lumbar DRGs. The net result is inhibition of p38 MAPK and p44/p42 MAPK activation, key enzymes involved in the phosphorylation (activation) of multiple ion channels. These include TRPV1 and its NGF-dependent increase in neuronal membrane expression, as well as voltage-gated sodium and calcium channels, all of which are implicated in the pathobiology of chronic pain. Although opioids are the gold standard for the treatment of cancer-related pain, control of pain associated with advanced PCa-induced bony metastases often requires high doses of opioid that in turn would be accompanied by numerous challenging adverse effects. Hence, small molecule AT_2R antagonists are worthy of further investigation as novel analgesics for relief of intractable bone pain associated with the advanced metastatic spread of PCa as well as for other difficult-to-control chronic pain states in which hyperalgesia worsens symptoms.

Acknowledgments

The authors would like to thank Dr Trent Woodruff, School of Biomedical Sciences, The University of Queensland, for helpful guidance to AM, and Dr Ai-Leen Lam and Ms Suzanne O'Hagan from the Centre for Integrated Preclinical Drug Development at The University of Queensland for their excellent technical assistance.

References

1 Ferlay J, Shin HR, Bray F, et al. Estimates of worldwide burden of cancer in 2008: GLOBOCAN 2008. Int J Cancer 2010;127:2893–917.

2 von Moos R, Strasser F, Gillessen S, Zaugg K. Metastatic bone pain: Treatment options with an emphasis on bisphosphonates. Support Care Cancer 2008;16:1105–15.

3 Muralidharan A, Wyse BD, Smith MT. Optimization and characterization of a rat model of prostate cancer-induced bone pain using behavioural, pharmacological, radiological, histological and immunohistochemical methods. Pharmacol Biochem Behav 2013;106:33–46.

4 Jimenez-Andrade JM, Mantyh WG, Bloom AP, et al. Bone cancer pain. Ann N Y Acad Sci 2010;1198:173–81.

5 Schmidt BL, Hamamoto DT, Simone DA, Wilcox GL. Mechanism of cancer pain. Mol Interv 2010;10:164–78.

6 Mantyh PW. Cancer pain and its impact on diagnosis, survival and quality of life. Nat Rev Neurosci 2006;7:797–809.

7 Muralidharan A, Smith MT. Pathobiology and management of prostate cancer-induced bone pain: Recent insights and future treatments. Inflammopharmacology 2013;21:339–63.

8 Smith MT, Woodruff TM, Wyse BD, Muralidharan A, Walther T. A small molecule angiotensin II type 2 receptor (AT2R) antagonist produces analgesia in a rat model of neuropathic pain by inhibition of p38 mitogen activated protein kinase (MAPK) and p42/p44 MAPK activation in the dorsal root ganglia. Pain Med 2013 Jun 6. [Epub ahead of print], doi: 10.1111/pme.12157.

9 Smith MT, Wyse BD, Edwards SR. Small Molecule Angiotensin II Type 2 receptor (AT2R) antagonists as novel analgesics for neuropathic pain: Comparative pharmacokinetics, radioligand binding and efficacy in rats. Pain Med 2013;14:692–705.

10 Porrello ER, Delbridge LM, Thomas WG. The angiotensin II type 2 (AT2) receptor: An enigmatic seven transmembrane receptor. Front Biosci 2009;14:958–72.

11 Yu L, Shao C, Gao L. Developmental expression patterns for angiotensin receptors in mouse skin and brain. J Renin Angiotensin Aldosterone Syst 2012 Nov 20. [Epub ahead of print], doi: 101177/1470320312467557.

12 Anand U, Facer P, Yiangou Y, et al. Angiotensin II type 2 receptor (AT(2) R) localization and antagonist-mediated inhibition of capsaicin responses and neurite outgrowth in human and rat sensory neurons. Eur J Pain 2013;17:1012–26.

13 Jimenez-Andrade JM, Bloom AP, Stake JI, et al. Pathological sprouting of adult nociceptors in chronic prostate cancer-induced bone pain. J Neurosci 2010;30:14649–56.

14 Halvorson KG, Kubota K, Sevcik MA, et al. A blocking antibody to nerve growth factor attenuates skeletal pain induced by prostate tumor cells growing in bone. Cancer Res 2005;65:9426–35.

15 Jimenez-Andrade JM, Ghilardi JR, Castaneda-Corral G, Kuskowski MA, Mantyh PW. Preventive or late administration of anti-NGF therapy attenuates tumor-induced nerve sprouting, neuroma formation, and cancer pain. Pain 2011;152:2564–74.

16 Ruiz G, Ceballos D, Banos JE. Behavioral and histological effects of endoneurial administration of nerve growth factor: Possible implications in neuropathic pain. Brain Res 2004;1011:1–6.

17 Mantyh PW, Koltzenburg M, Mendell LM, Tive L, Shelton DL. Antagonism of nerve growth factor-TrkA signaling and the relief of pain. Anesthesiology 2011;115:189–204.

18 Averill S, Delcroix JD, Michael GJ, et al. Nerve growth factor modulates the activation status and fast axonal transport of ERK 1/2 in adult nociceptive neurones. Mol Cell Neurosci 2001;18:183–96.

19 Ji RR, Samad TA, Jin SX, Schmoll R, Woolf CJ. p38 MAPK activation by NGF in primary sensory neurons after inflammation increases TRPV1 levels and maintains heat hyperalgesia. Neuron 2002;36:57–68.

20 Hudmon A, Choi JS, Tyrrell L, et al. Phosphorylation of sodium channel Na(v)1.8 by p38 mitogen-activated protein kinase increases current density in dorsal root ganglion neurons. J Neurosci 2008;28:3190–201.

21 Stamboulian S, Choi JS, Ahn HS, et al. ERK1/2 mitogen-activated protein kinase phosphorylates sodium channel Na(v)1.7 and alters its gating properties. J Neurosci 2010;30:1637–47.

22 Martin SW, Butcher AJ, Berrow NS, et al. Phosphorylation sites on calcium channel alpha1 and beta subunits regulate ERK-dependent modulation of neuronal N-type calcium channels. Cell Calcium 2006;39:275–92.

23 Basbaum AI, Bautista DM, Scherrer G, Julius D. Cellular and molecular mechanisms of pain. Cell 2009;139:267–84.

24 Zhang X, Huang J, McNaughton PA. NGF rapidly increases membrane expression of TRPV1 heat-gated ion channels. EMBO J 2005;24:4211–23.

25 Black JA, Nikolajsen L, Kroner K, Jensen TS, Waxman SG. Multiple sodium channel isoforms and mitogen-activated protein kinases are present in painful human neuromas. Ann Neurol 2008;64:644–53.

26 Persson AK, Gasser A, Black JA, Waxman SG. Nav1.7 accumulates and co-localizes with phosphorylated ERK1/2 within transected axons in early experimental neuromas. Exp Neurol 2011;230:273–9.

27 Ren K. An improved method for assessing mechanical allodynia in the rat. Physiol Behav 1999;67:711–6.

28 Hargreaves K, Dubner R, Brown F, Flores C, Joris J. A new and sensitive method for measuring thermal nociception in cutaneous hyperalgesia. Pain 1988;32:77–88.

29 Wood SJ, Slater CR. beta-Spectrin is colocalized with both voltage-gated sodium channels and ankyrinG at the adult rat neuromuscular junction. J Cell Biol 1998;140:675–84.

30 Wilkerson JL, Gentry KR, Dengler EC, et al. Immunofluorescent spectral analysis reveals the intrathecal cannabinoid agonist, AM1241, produces spinal anti-inflammatory cytokine responses in neuropathic rats exhibiting relief from allodynia. Brain Behav 2012;2:155–77.

31 McCarthy TD, Desem N, Kitson G, et al. Clinical Development of EMA401: An Angiotensin II Type 2 Receptor Antagonist as a Potential New Treatment for Neuropathic Pain. Abstracts of the 14th World Congress on Pain. Milan, Italy: IASP Press; 2012:31.

32 Patil J, Schwab A, Nussberger J, et al. Intraneuronal angiotensinergic system in rat and human dorsal root ganglia. Regul Pept 2010;162:90–8.

33 Zheng Q, Fang D, Cai J, et al. Enhanced excitability of small dorsal root ganglion neurons in rats with bone cancer pain. Mol Pain 2012;8:24.

34 Zhang JM, Strong JA. Recent evidence for activity-dependent initiation of sympathetic sprouting and neuropathic pain. Sheng Li Xue Bao 2008;60:617–27.

35 Devor M. Ectopic discharge in Abeta afferents as a source of neuropathic pain. Exp Brain Res 2009;196:115–28.

36 Gold MS, Flake NM. Inflammation-mediated hyperexcitability of sensory neurons. Neurosignals 2005;14:147–57.

37 Obata K, Yamanaka H, Kobayashi K, et al. Role of mitogen-activated protein kinase activation in injured and intact primary afferent neurons for mechanical and heat hypersensitivity after spinal nerve ligation. J Neurosci 2004;24:10211–22.

38 Obata K, Yamanaka H, Dai Y, et al. Activation of extracellular signal-regulated protein kinase in the dorsal root ganglion following inflammation near the nerve cell body. Neuroscience 2004;126:1011–21.

39 Ji RR, Baba H, Brenner GJ, Woolf CJ. Nociceptive-specific activation of ERK in spinal neurons contributes to pain hypersensitivity. Nat Neurosci 1999;2:1114–9.

40 Ji RR, Befort K, Brenner GJ, Woolf CJ. ERK MAP kinase activation in superficial spinal cord neurons induces prodynorphin and NK-1 upregulation and

contributes to persistent inflammatory pain hypersensitivity. J Neurosci 2002;22:478–85.

41 Jin SX, Zhuang ZY, Woolf CJ, Ji RR. p38 mitogen-activated protein kinase is activated after a spinal nerve ligation in spinal cord microglia and dorsal root ganglion neurons and contributes to the generation of neuropathic pain. J Neurosci 2003;23:4017–22.

42 Schafers M, Svensson CI, Sommer C, Sorkin LS. Tumor necrosis factor-alpha induces mechanical allodynia after spinal nerve ligation by activation of p38 MAPK in primary sensory neurons. J Neurosci 2003;23:2517–21.

43 Zhuang ZY, Gerner P, Woolf CJ, Ji RR. ERK is sequentially activated in neurons, microglia, and astrocytes by spinal nerve ligation and contributes to mechanical allodynia in this neuropathic pain model. Pain 2005;114:149–59.

44 Coulthard LR, White DE, Jones DL, McDermott MF, Burchill SA. p38(MAPK): Stress responses from molecular mechanisms to therapeutics. Trends Mol Med 2009;15:369–79.

45 Plouffe B, Guimond MO, Beaudry H, Gallo-Payet N. Role of tyrosine kinase receptors in angiotensin II AT2 receptor signaling: Involvement in neurite outgrowth and in p42/p44mapk activation in NG108-15 cells. Endocrinology 2006;147:4646–54.

46 Gendron L, Laflamme L, Rivard N, et al. Signals from the AT2 (angiotensin type 2) receptor of angiotensin II inhibit p21ras and activate MAPK (mitogen-activated protein kinase) to induce morphological neuronal differentiation in NG108-15 cells. Mol Endocrinol 1999;13:1615–26.

47 Stroth U, Blume A, Mielke K, Unger T. Angiotensin AT(2) receptor stimulates ERK1 and ERK2 in quiescent but inhibits ERK in NGF-stimulated PC12W cells. Brain Res Mol Brain Res 2000;78:175–80.

48 Hefti FF, Rosenthal A, Walicke PA, et al. Novel class of pain drugs based on antagonism of NGF. Trends Pharmacol Sci 2006;27:85–91.

49 Killock D. Experimental arthritis: NGF promotes synovial nerve sprouting. Nat Rev Rheumatol 2012;8:124.

50 Ro LS, Chen ST, Tang LM, Jacobs JM. Effect of NGF and anti-NGF on neuropathic pain in rats following chronic constriction injury of the sciatic nerve. Pain 1999;79:265–74.

51 Peleshok JC, Ribeiro-da-Silva A. Delayed reinnervation by nonpeptidergic nociceptive afferents of the glabrous skin of the rat hindpaw in a neuropathic pain model. J Comp Neurol 2011;519:49–63.

52 Chakrabarty A, Blacklock A, Svojanovsky S, Smith PG. Estrogen elicits dorsal root ganglion axon sprouting via a renin-angiotensin system. Endocrinology 2008;149:3452–60.

53 Izu Y, Mizoguchi F, Kawamata A, et al. Angiotensin II type 2 receptor blockade increases bone mass. J Biol Chem 2009;284:4857–64.

54 Sommer C, Lalonde A, Heckman HM, Rodriguez M, Myers RR. Quantitative neuropathology of a focal nerve injury causing hyperalgesia. J Neuropathol Exp Neurol 1995;54:635–43.

55 Kryger GS, Kryger Z, Zhang F, et al. Nerve growth factor inhibition prevents traumatic neuroma formation in the rat. J Hand Surg [Am] 2001;26:635–44.

56 Carmel M, Guimond MO, Battista MC, et al. Role of angiotensin II receptors in prostate cancer. Can Urol Assoc J 2008;2:282.

57 Chow L, Rezmann L, Imamura K, et al. Functional angiotensin II type 2 receptors inhibit growth factor signaling in LNCaP and PC3 prostate cancer cell lines. Prostate 2008;68:651–60.